



Traitement numérique de la singularité à l'axe pour les écoulements 3D en cavités tournantes

Noele Peres, Sébastien Poncet, Eric Serre

► To cite this version:

Noele Peres, Sébastien Poncet, Eric Serre. Traitement numérique de la singularité à l'axe pour les écoulements 3D en cavités tournantes. 20e Congrès Français de Mécanique, Aug 2011, Besançon, France. hal-00679104

HAL Id: hal-00679104

<https://hal.science/hal-00679104>

Submitted on 14 Mar 2012

HAL is a multi-disciplinary open access archive for the deposit and dissemination of scientific research documents, whether they are published or not. The documents may come from teaching and research institutions in France or abroad, or from public or private research centers.

L'archive ouverte pluridisciplinaire **HAL**, est destinée au dépôt et à la diffusion de documents scientifiques de niveau recherche, publiés ou non, émanant des établissements d'enseignement et de recherche français ou étrangers, des laboratoires publics ou privés.

Traitement numérique de la singularité à l'axe pour les écoulements 3D en cavités tournantes

N. Peres, S. Poncet et E. Serre

. Laboratoire de Mécanique, Modélisation et Procédés Propres (M2P2) IMT La Jetée, Technopôle de Château Gombert, 38 rue F. Joliot Curie 13451 Marseille, France

Résumé :

Le présent travail propose une méthode pour traiter la singularité en coordonnées cylindriques qui se pose dans le traitement des écoulements 3D confinés en rotation. La présente méthode consiste à discrétiser sur tout le diamètre $-R \leq r \leq R$ avec un nombre pair de noeuds dans la direction radiale. Dans la direction azimutale, le chevauchement des points de collocation et l'utilisation de conditions de parité sont évités en introduisant un décalage égal à $\pi/2K$ (K , le nombre de points de maillage dans cette direction) pour $\theta > \pi$ dans la transformée de Fourier. La convergence spectrale de la méthode est illustrée sur les solutions analytiques stationnaires et instationnaires. La capacité de la méthode numérique pour étudier les écoulements instationnaires complexes est illustrée sur deux configurations pour lesquelles des résultats expérimentaux ou numériques fiables sont disponibles dans la littérature.

Abstract :

The present work proposes a novel method to treat the cylindrical coordinate singularity which arises when dealing with three-dimensional confined rotating flows. In this work, we have developed a method which consists in discretizing the whole diameter $-R \leq r \leq R$ with an even number of radial Gauss-Lobatto nodes. In the azimuthal direction, the overlap in the discretization and especially the use of parity conditions are avoided by introducing a shift equal to $\pi/2K$ (K the number of mesh points in that direction) for $\theta > \pi$ in the Fourier transform. Spectral convergence of the method is illustrated on steady and unsteady analytical solutions. The ability of our numerical method to investigate complex unsteady flows is then illustrated for two rotating flow problems where other reliable experimental or numerical results are available in the literature.

Keywords : Rotating disk flows ; cylindrical coordinate singularity ; pseudo-spectral methods

1 Introduction

When simulating flows in cylindrical configurations such as pipe flows or rotating cavity flows, the main difficulty arises from the singularity, which appears on the axis. More generally, the singularity at the centerline of a cylindrical coordinate system is due to the presence of terms $1/r^n$ ($n = 1, 2$) in the Navier-Stokes equations governing the flow, where r is the radial distance. In the same time, the flow field itself does not have any singularity on the axis. Several numerical methods have been proposed in the literature [1] to overcome the singularities of the equations in cylindrical coordinates. Apparently these approaches depend greatly on whether a pseudo-spectral, finite-volume or finite-difference method is used, but in fact there are some similarities between them. Different methods have been developed in the past to avoid this singularity.

Mercader et al. [2] proposed recently an efficient spectral code used to study the Rayleigh-Bénard convection in a vertical stationary or rotating cylinder. To overcome the singularity on the axis they considered radial expansions in the diameter of the cell in order to avoid clustering about the axis, with a selected number of points to ensure that the origin is not a collocation point. Moreover, they

imposed implicitly some regularity conditions at $r = 0$ by forcing the proper parity of the Fourier expansions in the radial direction. This approach is named after Boyd [1] as unshifted Chebyshev polynomials of appropriate parity. The main advantages of their method are that it forces the minimal number of regularity conditions and that it reduces the size of the matrices.

In this paper, we present an efficient and accurate pseudospectral method to solve the time-dependent three-dimensional Navier-Stokes equations for some rotating flow arrangements. The adopted approach is based on the previous work of Heinrichs [3], who proposed two spectral collocation schemes to solve the Poisson problem on an unit disk. It consists first of mapping the domain $[0, 2\pi] \times [0, R]$ into $[0, 2\pi] \times [-R, R]$ and using an even number of mesh points in the radial direction as also prescribed by Mohseni and Colonius [4]. It ensures that no extra pole conditions have to be specified at the axis. An angular shift equal to $\pi/2K$ (K the number of mesh points in that direction) for $\theta > \pi$ in the discretization of angular direction is made to avoid an overlap of points and especially the use of parity conditions. To avoid the clustering of nodes around the rotation axis, a distribution of Gauss-Lobatto points is used. The flow is indeed laminar close to the rotation axis in most of the rotating flow applications, which does not require very thin meshes.

The paper is organized as follows: the numerical approach is presented in Section 2 together with the validation of the method against analytical steady and unsteady solutions in Section 3. To show the capability of the present method to simulate axisymmetric and non axisymmetric flows, it is applied in Section 4 to the study of the vortex breakdown phenomenon in a cylindrical cavity considering different configurations such as the first bifurcation in a rotor-stator cavity. Finally some concluding remarks and future views are provided in Section 5.

2 Numerical approach

The motion is governed by the incompressible three dimensional Navier-Stokes equations written in the velocity pressure formulation, together with the continuity equation and appropriate boundary conditions. A cylindrical polar coordinate system (r, θ, z) is used. The components of the velocity vector \mathbf{V} are denoted u , v and w in the (r, θ, z) directions respectively and P is the pressure. The scales for the dimensionless variables of space, time and velocity are h , Ω^{-1} and ΩR respectively, with h the interdisk spacing, R the outer radius of the rotating disk and Ω its rotation rate. The momentum equation, in dimensionless form, becomes:

$$\frac{\partial \mathbf{V}}{\partial t} + (\mathbf{V} \cdot \nabla) \mathbf{V} = -\nabla P + \frac{1}{Re} \Delta \mathbf{V} + \mathbf{F} \quad \text{in } D \quad (1)$$

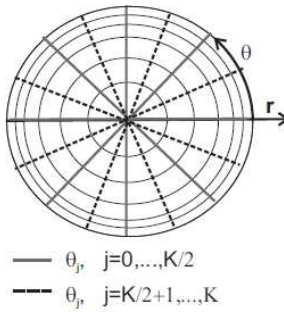
where \mathbf{F} represents a given body force. The continuity equation is given by $\nabla \cdot \mathbf{V} = 0$ in $\bar{D} = D \cup \Gamma$. The appropriate Dirichlet boundary conditions for the velocity vector write $\mathbf{V} = \mathbf{W}$ on $\Gamma = \partial D$.

We have considered two geometrical configurations for which the main flow depends on two non-dimensional parameters: the rotational Reynolds number Re and the aspect ratio G of the cavity defined as $Re = \Omega R^2 / \nu$ and $G = D/H$, where D and H are respectively the diameter and the height of the cavity, Ω the rotation rate of the rotating disk and ν the kinematic viscosity of the fluid.

The singularity at the junction of the stationary cylinder with the rotor is treated appropriately and the azimuthal velocity component has been regularized by employing a boundary layer function, $v = e^{\pm(z-1)/\mu}$, with $\mu = 0.006$ as described by Serre and Bontoux [5]. The numerical solution is based on a pseudo-spectral method with collocation Chebyshev polynomials in the radial r and axial z directions and Fourier collocation in the periodic azimuthal direction θ . The dimensionless space variables (\bar{r}, \bar{z}) have been normalized on $[-1, 1]$, a requisite for the use of Chebyshev polynomials. The normalized variables (r, z) satisfy the following relations $r = \bar{r}G$ and $z = \bar{z}$. The calculation domain is defined as $\bar{D} = (r, \theta, z) \in [-1, 1] \times [0, 2\pi] \times [-1, 1]$. In the two non-periodic directions, a Gauss-Lobatto distribution for the collocation points is used.

With respect to the azimuthal direction θ , the distribution of collocation points consists in the discretization of the whole diameter. To avoid an overlap of collocation points, in the azimuthal direction,

and especially the use of parity conditions, a shift equal to $\pi/2K$ for $\theta > \pi$ is introduced in the Fourier transform. For the derivatives in the azimuthal direction θ , the Fourier basis writes:



$$\Phi_k(\theta_j) = \begin{cases} \sin(k\theta_j) & \text{if } k = 1, \dots, \frac{K}{2} - 1, \\ \cos\left(\frac{K}{2}\theta_j\right) + \sin\left(\frac{K}{2}\theta_j\right) & \text{if } k = \frac{K}{2}, \\ \cos\left(\left(k - \left(\frac{K}{2} + 1\right)\right)\theta_j\right) & \text{if } k = \frac{K}{2} + 1, \dots, K. \end{cases} \quad (2)$$

The Navier-Stokes equations are discretized in time by using a semi-implicit scheme that combines an implicit second order Euler scheme for the diffusive terms and an explicit Adam-Bashforth scheme for the convective non-linear terms. The solution method is based on an efficient projection scheme and is a modification of the projection method initially proposed by Goda as described in [6]. For the computation of the non-linear terms, the derivatives in each space direction are calculated in the spectral space and the products are performed in the physical one. The connection between the two spaces is made through the use of a Fast Fourier Transform algorithm for the radial and axial directions and through a matrix multiplication in the azimuthal direction. For the diffusion terms the derivatives are performed in physical space using a simple matrix multiplication. Finally, all the resulting Helmholtz and Poisson problems are solved using a full diagonalization technique for each Fourier mode.

3 Validation against analytical solutions

The accuracy of the method is checked on the exact steady and time-dependent solutions defined in $\bar{D} = [-1, 1] \times [0, 2\pi] \times [-1, 1]$. The results presented here have been obtained for $G = 10$ and $Re = 250$. The space accuracy of the method is evaluated by computing the discrete errors at the inner collocation points Er , see [6] for more details. In the steady case, the time step used is $\delta t = 5 \times 10^{-3}$ and the values of the error for the velocity component u and for the pressure P are represented in figures 1(a) and 1(b) respectively. An exponential decay with the number of mesh points is obtained, which is characteristic of spectral methods.

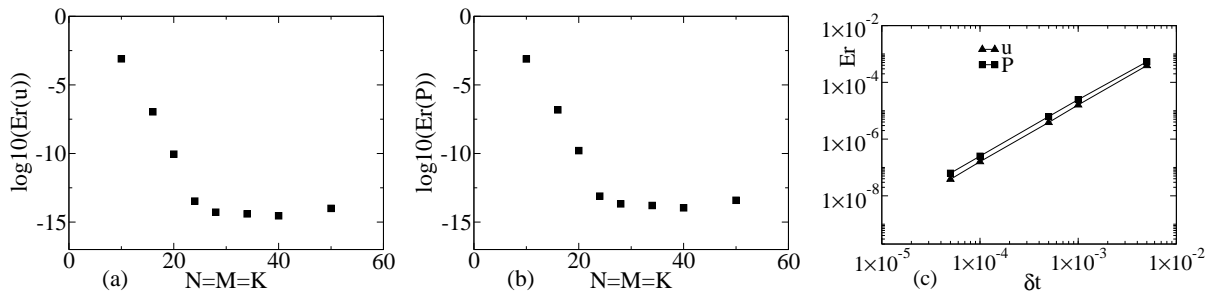


Figure 1: Evolution of the error, $\log_{10}(Er)$, for the velocity component u and for the pressure P versus the polynomial degrees $N = M = K$ (a,b) and Er versus time step (c).

Figure 1(c) represents the values of the error for the radial velocity component u and for the pressure P considering the time-dependent solution. The time step was decreased from $\delta t = 5 \times 10^{-3}$ to $\delta t = 5 \times 10^{-5}$ and the polynomial degrees are fixed to 40 for each space direction. The results are in line with the results obtained by Raspo et al [6], showing that the code is second-order accurate in time $O(\delta t^2)$ for the radial velocity component and for the pressure inside the computational domain. The same temporal behavior was observed for the azimuthal and axial velocity components.

4 Results

The results obtained are compared to other reliable data available in the literature in two cases: the vortex breakdown phenomenon in a stationary cylinder driven by a rotating top disk considered by Serre & Bontoux [5] using DNS for different aspect ratios and the non axisymmetric flow in a rotor-stator cavity at a transitional Reynolds number [7, 8].

4.1 Vortex breakdown phenomenon in a cylinder with a rotating top disk

Vortex breakdown and transition to time-dependent regimes are initially investigated in a stationary cylinder with a rotating top disk. Two simulations are carried out. The first calculation for $Re = 1850$ and $G = 1$ is performed using a $126 \times 8 \times 126$ mesh grid in the radial, azimuthal and axial directions respectively with a time step equal to 10^{-2} . The second simulation was done using the same time step and grid arrangement but for $G = 0.8$ and $Re = 2750$.

In the first case, the base flow is laminar and axisymmetric. The iso-surface $w = 0$ of the axial velocity is presented in figure 2(a), showing that the flow is clearly axisymmetric. It highlights also the presence of an axisymmetric vortex breakdown along the rotation axis with two bubbles, which confirm previous experimental and numerical results (Fig. 2(b)). The present results are found in quite good agreement with the previous ones for the bubble characteristics defined in Fig. 2(c), even if the method is not optimized to simulate flow phenomenon close to the axis, where the grid is coarser.

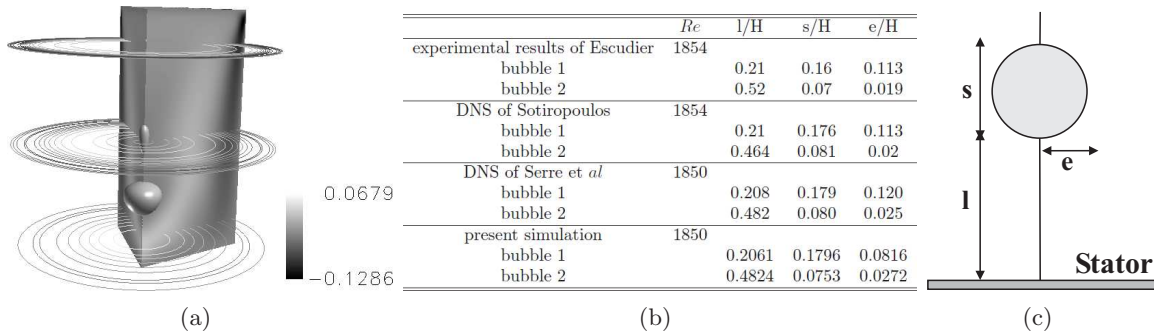


Figure 2: Axial velocity w for $Re = 1850$ and $G = 1$: (a) iso-contours at different axial positions with the iso-values $w = 0$; (b) comparison of the bubble characteristic lengths; (c) schematic representation of the bubble characteristic lengths.

Concerning the case for $Re = 2750$ and $G = 0.8$, the flow gets unsteady as shown in Figure 3. The bubble is stretched by the shear along the axis and then is splitted into two bubbles, which finally merge, confirming the results described in [5]. We can deduce the time period of oscillations of the two bubbles. In the present case, the dimensionless time period is $36.2\Omega^{-1}$ to be compared to the values $36\Omega^{-1}$ of Stevens et al. [9] for $Re < 3500$ and $55.6\Omega^{-1}$ obtained by Serre & Bontoux [5].

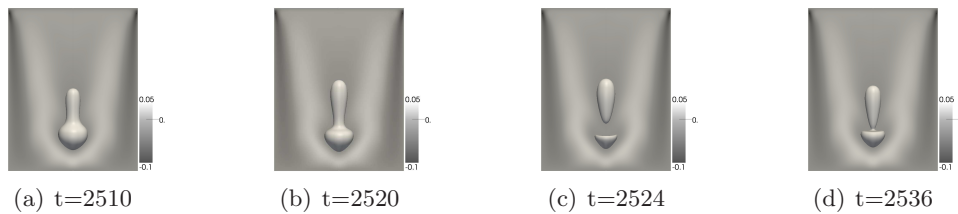


Figure 3: Iso-surfaces of $w = 0$ and iso-contours of w in a (r, z) plane for $Re = 2750$ and $G = 0.8$.

Finally with the aim to show the capability of the method to compute non axisymmetric flows was made a third case for $G = 0.5$ and $Re = 6500$. A $126 \times 48 \times 65$ mesh grid in the radial, azimuthal and axial directions respectively has been used together with a time step equal to 10^{-2} . The results presented in Figure 4 confirms the expected three-dimensional nature of the flow. The surface identified

as the breakdown zone ($w = 0$) (Fig. 4) has changed the bubble form having now a S-shaped form corresponding to the regime defined by Escudier [10] as the precession regime of the lower breakdown structure. This behavior is due to the interaction of the vortex-breakdown with the structures from the vertical wall boundary layer as described in [11].

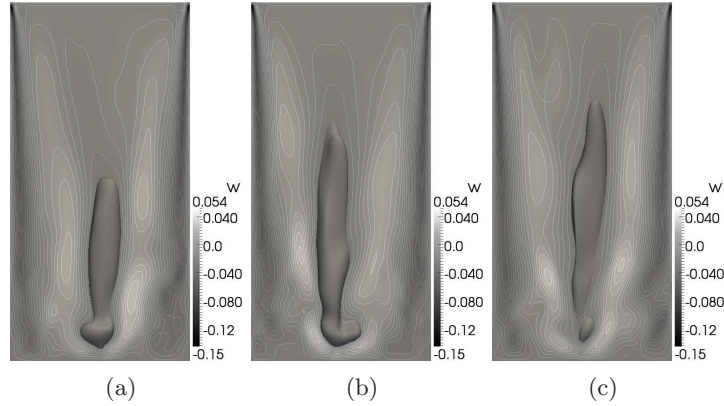


Figure 4: Iso-surface ($w = 0$) and iso-lines of the axial component of velocity w for $G = 0.5$ and $Re = 6500$: (a) $t = 2100 \Omega^{-1}$, (b) $t = 2292 \Omega^{-1}$ and (c) $t = 2484 \Omega^{-1}$.

4.2 Batchelor rotor-stator flows at a transitional Reynolds number

Some computations have been also performed in a rotor-stator cavity of large aspect ratio $G = 17.45$ for two Reynolds numbers $Re = 10000$ and $Re = 20900$. For this set of parameters, the flow exhibits a Batchelor flow structure with separated boundary layers [7, 8]. The results have been obtained using $126 \times 128 \times 33$ collocation points in the radial, azimuthal and axial directions respectively with a time step equal to 10^{-3} . Some flow visualizations in the stator boundary layer are presented in Figure 5.

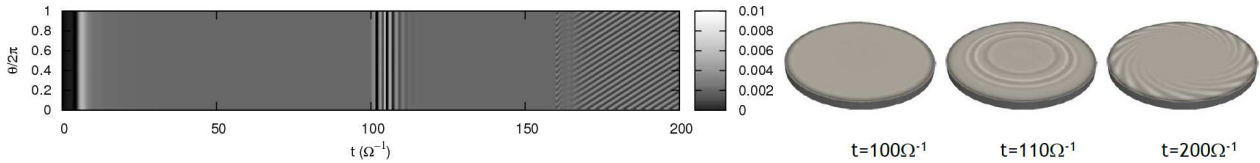


Figure 5: Axial velocity w : space-time diagram ($\bar{z} = -0.773$ and $\bar{r} = 0.809$); (r, θ) planes in the stator boundary ($\bar{z} = -0.773$) layer for $G = 17.45$: ($t = 100 \Omega^{-1}$, $Re = 10000$), ($t = 110 \Omega^{-1}$, $Re = 20900$), ($t = 200 \Omega^{-1}$, $Re = 20900$).

Schouveiler et al. [8] have shown experimentally that the flow remains laminar until the appearance of circular rolls (CR) in the stator boundary layers for $Re \geq 10500$. These patterns coexist in the experiments with spiral rolls, denoted SR1, for $Re \geq 20000$. These spirals are located at the periphery of the cavity, also along the stator side. Poncet et al. [7] performed DNS results in an annular cavity and obtained only the spiral patterns for this range of parameters, the circular rolls being observed only in a transient state. In the present case, the cavity is cylindrical and the results obtained are in perfect agreement with Poncet et al. [7] and in good agreement with the experimental results of Schouveiler et al. [8]. The circular rolls are here also observed only in a transient state with a dimensionless time period of $2.1\Omega^{-1}$ after increasing the Reynolds number from 10000 to 20900 at $t = 100 \Omega^{-1}$. The mode $K = 17$ is then perturbed with an amplitude of 5% at $t = 160 \Omega^{-1}$ to accelerate the transition to the spiral regime. 17 stationary spiral rolls are thus obtained with a dimensionless time period of $3\Omega^{-1}$. Schouveiler et al. [8] showed experimentally that the mode 18 is the most unstable. This weak discrepancy on the number of spiral arms can be explained by the fact that this instability is an Eckhaus instability. Thus, the number of arms is very sensitive to the time history of the flow and to the perturbations, which have been introduced experimentally or numerically. The present 17 spiral arms roll up in the sense of rotation of the rotor and form thus a positive angle with the tangential direction equal to $\varepsilon = 25^\circ$, which fully matches with [7, 8].

5 Conclusions

A novel method has been developed to take into account the axis singularity, which appears when using cylindrical coordinates within a rotating cavity. This method ensures that no extra pole conditions have to be specified at the axis. It has been first validated against analytical steady and unsteady solutions, while preserving the spectral accuracy. Then two different configurations have been used to test the method: the vortex breakdown phenomenon [5, 11] and the two first bifurcations in a rotor-stator cavity [7, 8]. For these two cases, the main characteristics of the mean flow and the instabilities have been favorably compared with the previous works, showing the capability of the method to predict with accuracy both axisymmetric and non-axisymmetric, steady and unsteady flows. The code has been recently extended for the simulation of turbulent flows using a “no-model” LES approach (Séverac & Serre [12]). Some calculations are in progress in the rotor-stator cavity considered by Craft *et al.* [13] to highlight the presence of 3D large scale vortices embedded in the turbulent flow. It has been shown recently (private communication) that those patterns are very sensitive to the presence or not of a hub rotating with the rotor. They have been indeed observed only in the cylindrical case and not in the annular one. The new method is then absolutely necessary and appears moreover particularly well adapted to simulate such flows as the patterns are located far from the rotation axis, where the grid is coarser.

References

- [1] J. P. Boyd. *Chebyshev and Fourier Spectral Methods, 2th Edition*. Dover Publications, 2001.
- [2] I. Mercader, O. Batiste, and A. Alonso. An efficient spectral code for incompressible flows in cylindrical geometries. *Comput. Fluids*, 39:215–224, 2010.
- [3] W. Heinrichs. Spectral collocation schemes on the unit disc. *J. Comp. Phys.*, 199:66–86, 2004.
- [4] K. Mohseni and T. Colonius. Numerical treatment of polar coordinate singularities. *J. Comp. Phys.*, 157:787–795, 2000.
- [5] E. Serre and P. Bontoux. Vortex breakdown in a three-dimensional swirling flow. *J. Fluid Mech.*, 459:347–370, 2002.
- [6] I. Raspo, S. Hugues, E. Serre, A. Randriamampianina, and P. Bontoux. A spectral projection method for the simulation of complex three-dimensional rotating flows. *Comput. Fluids*, 31:745–767, 2002.
- [7] S. Poncet, E. Serre, and P. Le Gal. Revisiting the two first instabilities of the flow in an annular rotor-stator cavity. *Phys. Fluids*, 21 (6):064106, 2009.
- [8] L. Schouveiler, P. Le Gal, and M.P. Chauve. Stability of a traveling roll system in a rotating disk flow. *Phys. Fluids*, 10:2695–2697, 1998.
- [9] J. L. Stevens, J. M. Lopez, and B. J. Cantwell. Oscillatory flow states in an enclosed cylinder with a rotating endwall. *J. Fluid Mech.*, 389:101–118, 1999.
- [10] M. P. Escudier. Observations of the flow produced in a cylindrical container by a rotating end wall. *Exps. Fluids*, 2:176–186, 1984.
- [11] E. Serre and P. Bontoux. Three-dimensional swirling flow with a precessing vortex breakdown in a rotor-stator cylinder. *Phys. Fluids*, 13:3500–3503, 2001.
- [12] E. Séverac and E. Serre. A spectral vanishing viscosity for the LES of turbulent flows within rotating cavities. *J. Comp. Phys.*, 226:1234–1255, 2007.
- [13] T. J. Craft, H. Iacovides, B. E. Launder, and A. Zacharos. Some swirling flow challenges for turbulent CFD flow. *Flow, Turb. Combust.*, 80:419–434, 2008.